Journal of the Korean Nuclear Society
Volume 32, Number 4, pp.379~394, August 2000

Sensitivity Studies on Thermal Margin of Reactor Vessel Lower Head During a Core Melt Accident

Chan-Soo Kim and Kune Y. Suh
Seoul National University
San 56-1 Shinrim-dong, Kwanak-gu, Seoul, 151-742, Korea
kysuh@plaza.snu.ac.kr

(Received May 15, 2000)

Abstract

As an in-vessel retention (IVR) design concept in coping with a severe accident in the nuclear power plant during which time a considerable amount of core material may melt, external cooling of the reactor vessel has been suggested to protect the lower head from overheating due to relocated material from the core. The efficiency of the ex-vessel management may be estimated by the thermal margin defined as the ratio of the critical heat flux (CHF) to the actual heat flux from the reactor vessel. Principal factors affecting the thermal margin calculation are the amount of heat to be transferred downward from the molten pool, variation of heat flux with the angular position, and the amount of removable heat by external cooling. In this paper a thorough literature survey is made and relevant models and correlations are critically reviewed and applied in terms of their capabilities and uncertainties in estimating the thermal margin to potential failure of the vessel on account of the CHF. Results of the thermal margin calculation are statistically treated and the associated uncertainties are quantitatively evaluated to shed light on the issues requiring further attention and study in the near term. Our results indicated a higher thermal margin at the bottom than at the top of the vessel accounting for the natural convection within the hemispherical molten debris pool in the lower plenum. The information obtained from this study will serve as the backbone in identifying the maximum heat removal capability and limitations of the IVR technology called the Corium Attack Syndrome Immunization Structures (COASISO) being developed for next generation reactors.

Key Words : in-vessel retention (IVR), critical heat flux (CHF), thermal margin, external cooling, core melt accident, COASISO

1. Introduction

A wide spectrum of management strategies were proposed to cope with a nuclear reactor severe accident in which a massive amount of core material may possibly melt and move down to the lower plenum of the reactor vessel. As a viable means to ensure adequate cooling of the decay

heat generating debris bed and the retaining vessel wall, the so-called IVR-EVC (in-vessel retention through external vessel cooling) appears to draw a keen attention from the nuclear safety community. The IVR-EVC strategy certainly manifests itself a highly promising potential to prevent the vessel failure by providing with reliable heat removal mechanisms during a severe accident. As quantitative analysis as may reasonably be performed is prerequisite to estimating the thermal margin of the reactor vessel wall containing the exceedingly high temperature core material when the IVR-EVC design is considered in the next-generation reactors as well as already operating nuclear power plants. In this study the thermal margin is defined as the ratio of the critical heat flux (CHF) value to the local downward heat flux considering the natural convection effect within the molten pool.

Boiling has long been recognized as one of the most efficient ways of cooling hot or heated surfaces, which is of fundamental importance in many applications in the nuclear and chemical industries. However, most of boiling research was focused on upward facing geometry and performed in the experiments using small objects. Thus there is a scarcity of data with direct applicability to cooling the hemispherical reactor lower head externally on a major scale. Recently, a few number of studies did examine the external cooling of nuclear reactor vessel downward facing hemispherical surface. In this regard, buoyancy-driven turbulent natural convection with internal heat generation in the high Rayleigh number was recognized as the heat transfer mechanism in the molten debris pool. Again, there exists virtually no predictive model to allow for comprehensive analysis of the buoyancy-driven high Rayleigh number turbulent natural convection, nor relevant experimental database for the precise mechanisms involving the process. In this regard, any extrapolation to different geometries and convection conditions will have to be considered with certain reservations and care.

Special design features to facilitate rapid flooding are essential to the success of the IVR. The so-called Corium Attack Syndrome Immunization Structures (COASIS) are being developed at the Seoul National University as prospective in-vessel retention devices for a next-generation water reactor in concert with existing ex-vessel management measures [1]. Both the engineered gap structures inside the vessel (COASISI) and outside the vessel (COASISO) were demonstrated to maintain effective heat transfer geometry during molten core debris attack when applied to the TMI-2 and the Korean Standard Nuclear Plant (KSNP) reactor cases.

Guo and El-Genk [2] performed an experimental study of saturated pool boiling from the downward facing and inclined surface. Pool boiling curves for inclinations of 0°, 5°, 10°, 15°, 30°, 45°, and 90° were obtained by quenching a 12.8mm thick copper disk having a diameter of 50.8mm in a pool of saturated water. Results showed that nucleate boiling heat flux decreases as angle of inclination is increased. However, the decrease in nucleate boiling heat flux with inclination is more pronounced at the lower wall superheat, increasing with surface inclination. The inclination angle is 90° at the vertical plate and 0° at the downward plate.

El-Genk and Glebov [3] studied transient pool boiling from downward facing curved surfaces. In this study, quenching experiments were performed to investigate the effects of wall thickness on pool boiling from downward facing curved surfaces in water.

Theofanous and Syri [4] performed several external cooling experiments at the ULPU facility. Their experiments were divided into configurations

I, II, and III. Configuration I experiment established the lower limits of coolability under lower submergence, pool boiling conditions. Using configuration II experiments, they considered the heat flux shape, full submergence and natural circulation in the reactor lower head.

Rouge et al. [5] performed the SULTAN experiment at six campaigns. Each campaign has one inclination angle and gap of the channel at various conditions of the pressure, mass flux and inlet subcooling. They suggested the CHF correlation considering the gap size, pressure, quality, mass flux and inclination angle, and utilized the CATHARE thermal hydraulic code to interpret the data and extrapolate to the real geometry.

Park and Jeong [6] calculated the thermal margin for external reactor vessel cooling in a large, advanced light water reactor (ALWR). They chose Steinberner and Reineke' s [7] Nusselt number for the upward natural convection and Theofanous et al.' s [8] Nusselt number and Mayinger et al.' s [9] Nusselt number for the downward convection, respectively. They also cited the correlation based on the Mini-ACOPO experimental data to find the angular heat flux distribution and obtained the CHF at the outer surface of the lower head using Theofanous et al.' s [8] correlation developed from the ULPU-2000 configuration II experiment. Their results showed that the thermal margins were 1.27 and 1.64 depending on which correlation was used at the highest angle of the debris, i.e. 85° measured from the bottom of the vessel.

In this study we examine the principal factors affecting the thermal margin calculation such as the amount of heat to be transferred downward from the molten pool, variation of heat flux with the angular position, and the amount of removable heat by external cooling. Relevant models and correlations are reviewed in terms of their capabilities and uncertainties in estimating the thermal margin to failure of the vessel on account of the CHF. Results of the thermal margin calculation are statistically treated and the associated uncertainties are quantitatively assessed to identify the remaining issues to be resolved in the near term during the course of engineering design of COASISO for the IVR of next generation reactors.

2. Model Description

In this section we mainly elucidate the factors affecting the thermal margin calculations for the reactor vessel. Figure 1 schematically shows the COASISO hemispherical shell structure for heat removal from the reactor vessel lower head considered mainly and uniquely in this study in assessing the IVR capability for next generation reactors. The basic factors influencing the thermal margin calculation are the amount of heat to be

Table 1. Correlations and Cases Considered in This Study

Natural Convection Correlation	Azimuthal Heat Flux Correlation	CHF Correlation	Mass Flow Rate (kg/s)	Initial Sub-cooling (K)	Pressure (MPa)	Gap Size (m)	Vessel Radius (m)
Theofanous et al.* [8]	Theofanous et al. [8]	Theofanous & Syri [4]	25	0*	0.12	0.05	2
Mayinger et al. [9]	Park et al. [13]	Rouge et al.* [5]	50	10	0.2*	0.10	2.5*
Kelkar & Patankar [11]	Suh & Henry* [14]	Cheung et al. [10]	100	50	0.3	0.15*	
	Asfia & Dhir [15]		200*				
			300				

* the reference case

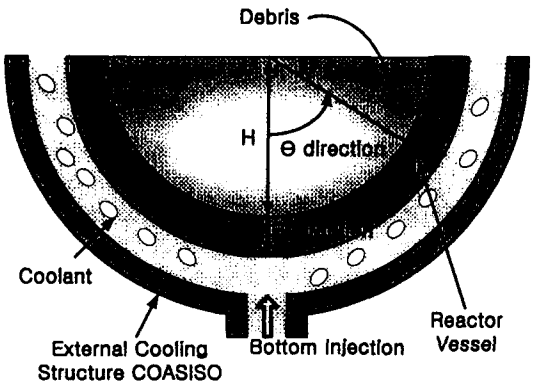

Fig. 1. Schematic Diagram for COASISO

transferred downward from the debris pool, the azimuthal variation of local heat flux from the downward surface, and the amount of removable heat by the external cooling of the vessel. The first two factors arise from the natural convection within the molten pool of debris, while the last factor results from the heat removal capability of the injected or flooded water outside the reactor vessel lower head. To estimate the thermal margin, we used the information readily available in the literature for the first two factors, and calculated the CHF values for the last factor utilizing Theofanous and Syri' s [4], Rouge et al.' s [5] and Cheung et al.' s [10] correlations. Table 1 presents relevant correlations and the cases considered in this study.

2.1. Natural Convection Effect

To estimate the thermal margin, we first need the amount of heat transferred to the vessel from the internal pool. The amount of heat source is determined from the decay heat, which is dependent on shutdown time, the amount of heat transferred downward by the natural convection, and the azimuthal variation of the downward heat flux. In this study we chose to use the decay power of 26 MW in the molten pool given by Park and Jeong [6].

To investigate the amount of heat transferred downward by natural convection we examined five reference correlations available in the literature [7,8,9,11,12] collected in Table 2. Despite a great deal of studies performed so far, most of the data were taken from experiments with relatively low

Table 2. Summary of Natural Convection Correlations

Geometry	Correlation	Ra'	Pr	Reference Type of data
Rectangular	**up-** $Nu=0.345Ra'^{0.233}$ **side-** $Nu=0.85Ra'^{0.19}$ **down-** $Nu=1.389Ra'^{0.095}$	1×10^{7} to 1×10^{14}	7	Steinberner & Reineke[7] Experimental
Semicircular	**up-** $Nu=0.4Ra'^{0.2}$ **side-** $Nu=0.55Ra'^{0.2}$	7×10^{6} to 5×10^{14}	7	Mayinger et al.[9] Numerical
Hemispherical	**up-** $Nu=0.345Ra'^{0.233}$ **down-** $Nu=1.389Ra'^{0.095}$	1×10^{12} to 1×10^{15}	2.5 to 11	Theofanous et al.[8] Experimental
Hemispherical	**up-** $Nu=0.185Ra'^{0.237}$ **down-** $Nu=0.1Ra'^{0.25}$	1×10^{6} to 1×10^{16}	1	Kelkar & Patankar[11] Numerical
Torispherical	**up-** $Nu=0.345Ra'^{0.233}$ **side-** $Nu=0.85Ra'^{0.19}$ **down-** $u=0.54Ra'^{0.18}(H/R)^{0.26}$	1×10^{14} to 1×10^{15}	7	Kymalainen et al.[12] Experimental

Rayleigh number (Ra') as compared to a postulated severe accident condition for which Ra' may well exceed 1×10^{17}. In these references Ra' is normally defined as

$$Ra' = \frac{g\beta Q_v H^5}{k_p \alpha_p \nu_p} \quad (1)$$

where the subscript p denotes the pool.

A wide spectrum of data were taken from different geometries of rectangular, semicircular, hemispherical and torispherical pool. Some of the data were obtained from experiments while the other data were derived from numerical studies. Utilizing the natural convection correlations for the downward heat transfer (Nu_{dn}) versus the upward heat transfer (Nu_{up}) the downward heat split fraction was calculated as follows.

$$frac = \frac{Nu_{dn} 2\pi r^2}{Nu_{dn} 2\pi r^2 + Nu_{up} \pi r^2} = \frac{2 Nu_{dn}}{2 Nu_{dn} + Nu_{up}} \quad (2)$$

Considering the reactor vessel lower head geometry, we chose to employ the three correlations [8, 9, 11] for the semicircular or hemispherical pool in which the sideward heat transfer is not accounted for separately from the downward heat transfer. Figure 2 shows the values of the heat split fraction according to the different correlations.

For all the experimental studies carried out so far we assumed that the heat flux from the debris

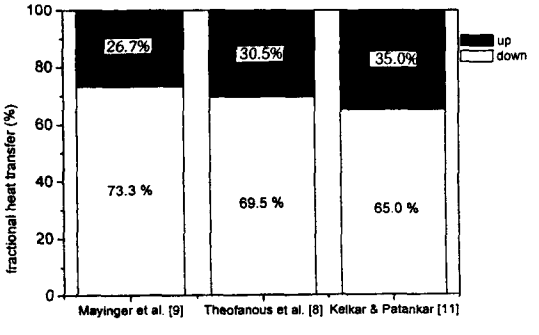

Fig. 2. Heat Split Fraction for Different Correlations

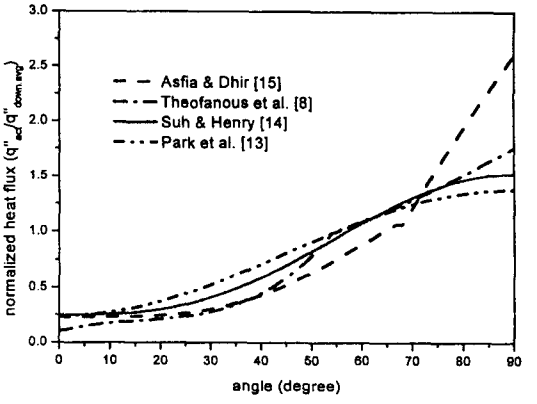

Fig. 3. Azimuthal Variation of Heat Flux in Natural Convection

bed to the vessel wall varies azimuthally. For years a number of investigators [8,13,14,15] have studied the heat flux from the debris to the reactor vessel lower head. They concentrated on several natural convection experiments in the lower head vessel. In this study we need correlations for the heat transfer coefficient varying with the local position, which are compared in Fig. 3.

2.2. Heat Removal by External Cooling

The main factor in calculating the thermal margin is the heat removal capacity of the external cooling water. Generally this capacity is represented by the CHF, which is the value for a maximum heat removal by water.

Theofanous and Syri' s [4] CHF correlation developed from the ULPU-2000 configuration II experiment reads in kW/m^2

$$q''_{CHF}(\theta) = 490 + 30.2\theta - 8.88\times10^{-1}\theta^2 + 1.35\times10^{-2}\theta^3 - 6.65\times10^{-5}\theta^4 \quad (3)$$

As the experimental apparatus for the ULPU-2000 configuration II was set up as a closed loop, the above equation yielded the CHF value for the case of forced convective boiling induced by buoyancy-driven natural circulation.

The second one is Cheung et al.' s [10] result. They established a scaling law to develop a design correlation for prediction of the CHF on the exterior surface of a real-size reactor vessel. Their correlation takes the following form:

$$q''_{CHF} = F_{L_b} F_P F_\theta F_{Ja} \tag{4}$$

The correlation consists of the four functions. The function F_{L_b} is a size correction factor depending on the vessel size and local azimuthal position. The value for depends on the fluid properties varying with the system pressure. The spatial variation function F_θ is a least-squares fit, which varies within $\pm 5\%$. The function F_{Ja} depends on the subcooling due to local liquid head.

The other one is Rouge et al.' s [5] correlation based on the 191 CHF data from the SULTAN facility. This correlation includes the local thermodynamic quality (x), gap (e) in m, pressure (p) in MPa, heat flux in MW/m^2, mass flux (G) in kg/m^{2}s and inclination angle (θ) measured from the horizontal line.

$$\begin{aligned}
q''_{CHF} &= A0(e,p,G) + A1(e,G)x + A2(e,p,G,x)x^2 \\
&\quad + A3(e,p,G,x)\sin\theta + A4(e,p,G,x)\sin^2\theta \\
A0 &= b0 + b1\times e\times \ln G + b2/p^2 + b3\times G + b4\times e/p + b5\times e/p^2 + b6\times p\times (\ln G)^2 \\
A1 &= b7\times (\ln G)^2 + b8\times e\times \ln G, \quad A2 = b9\times e \\
A3 &= b10\times (\ln G)^2 + b11\times e\times p + b12\times x\times \ln G \\
A4 &= b13\times p + b14\times \ln G + b15\times x + b16\times e \\
b0 &= 0.65444,\ b1 = -1.2018,\ b2 = -0.008388,\ b3 = 0.000179,\ b4 = 1.36899 \\
b5 &= -0.077415,\ b6 = 0.024967,\ b7 = -0.086511,\ b8 = -4.49425 \\
b9 &= 9.28489,\ b10 = -0.0066169,\ b11 = 11.62546,\ b12 = 0.855759 \\
b13 &= -1.74177,\ b14 = 0.182895,\ b15 = -1.8898,\ b16 = 2.2636
\end{aligned} \tag{5}$$

The standard deviation is 9.7% in the correlation. In this study, the mass flux and the quality at the azimuthal positions were respectively calculated as follows:

$$G = \dot{m} / A_{channel}(\theta) \tag{6}$$

$$x(\theta) = \left(h_{in} + \int_0^\theta \frac{q''_{act}(\theta)}{\dot{m}} A_{heated}(\theta) d\theta - h_f \right) / h_{fg} \tag{7}$$

As presented in Table 1, we assumed the uniform gap sizes of 5, 10 and 15 cm between the COASISO hemispherical shell structure and the reactor vessel. The coolant is supplied to the COASISO under the pressure of 0.12, 0.2, and 0.3 MPa. We assumed that the thermodynamic quality in the subcooled boiling region is zero. The subcooling effect on the CHF is not explicitly considered in Rouge et al.' s correlation. The coolant mass flow rate is assumed to be 25, 50, 100, 200 and 300 kg/s in this study.

3. Results and Discussion

The results cover a wide spectrum of sensitivity analyses varying the CHF correlation, mass flow rate and the initial subcooling of the external vessel coolant, vessel radius, the fraction of downward heat transfer, and the correlations for the azimuthal distribution of downward heat flux. If there is no special mention, the parameters are fixed for the reference case specified as follows:

- critical heat flux correlation: Rouge et al. [5]
- mass flow rate of the external vessel coolant: 200 kg/s
- initial subcooling of the external vessel coolant: 0 K
- vessel outer radius: 2.5 m
- fraction of downward heat transfer: 69.5% according to Theofanous et al. [8]
- azimuthal distribution of downward heat flux: Suh and Henry [14]
- gap size between the COASISO shell structure and the reactor vessel: 15 cm
- pressure of the coolant: 0.2 MPa

- decay power in the molten pool: 26 MW according to Park and Jeong [6]

Figure 4(a) shows the CHF values determined alongside the outer surface of the vessel utilizing different correlations [4,5,10]. The CHF values are generally observed to increase with the angular position from the bottom (θ = 0°) to the top (θ = 90°) as more heat can be removed from the vertical heated surface than from the downward facing, inclined heated surface by virtue of the gravity-driven flow effect. Cheung et al.' s [10] CHF values considering the local liquid head, which in turn gives rise to additional subcooling, are higher than those without the hydrostatic pressure increase effect. Cheung et al.' s values for the saturated pool boiling envelop Theofanous and Syri' s [4] results considering the natural circulation alongside the outer vessel, and Rouge et al.' s [5] values accounting for the forced convection except at the very top and at the bottom. The lower CHF values for Rouge et al.' s at the bottom accounts for the smaller gap size than in the other experiments. After that point the CHF value increases with the azimuthal angle of the vessel. The CHF is leveled off and is slightly decreased at the top, say θ = 80°~90°, because the flow quality is increased.

Table 3 presents the azimuthally varying CHF values utilizing the four correlations, which generally vary from 0.7 to 1.5 MW/m2. Observe that because of the relatively small gap size and flat surface the CHF values of Rouge et al.' s correlation are smaller than those of Theofanous and Syri' s [4] and Cheung et al.' s [10] at the bottom. However, Cheung et al.' s experiments with thermal insulation referenced by Yang et al. [16] show that the CHF values are larger than the other experimental values on account of the flow mixing and three-dimensional curvature effect. Unfortunately, however, Rouge et al.' s [5] correlation turns out to be the only one at the moment to be applied to the COASISO structure because this is the one correlation considering the gap size, pressure, azimuthal angle, local quality and local mass flux in the inclined channel for the downward facing heated surface. Rouge et al' s [5] CHF correlation may not be applied in the bottom region where the effect of curved surface is prominent and the flow field is unstable with bottom injection, however. The correlation may rather be reliably applied in the region where the surface curvature and flow developing effects are diminished. The critical heat flux ratio (CHFR) defined as the CHF divided by the actual heat flux is relatively high at the bottom so that the bottom region is in thermally safe region. We thus mainly mention the CHF and CHFR at the top where the thermal load gets large. Cheung et al' s [10]

Table 3. CHF Values* for Different Correlations

Angular Position	30°	40°	50°	60°	70°	80°	90°
Rouge et al. [5] (200 kg/s, 0.2 MPa, gap size:0.15m)	0.733	0.921	1.097	1.245	1.351	1.405	1.404
Cheung et al. [10] (w/ local liquid head)	1.123	1.248	1.327	1.390	1.428	1.442	1.435
Theofanous & Syri [4]	0.907	0.978	1.052	1.159	1.287	1.410	1.494
Cheung et al. [10] (w/o local liquid head)	0.739	0.830	0.886	0.945	0.990	1.022	1.041

* unit: MW/m^2

correlation can be applied in the limited case of pool boiling without the natural recirculation effect. In addition, Theofanous and Syri' s [4] correlation can be applied for a specific condition of the AP-600 like geometry.

Figure 4(b) depicts the associated CHFR utilizing the four correlations. It is shown that, given the thermal load, the CHFR can approach unity at the top so that the vessel might have only marginal safety at the top of the lower head where the focusing effect of the metal layer may further aggravate the situation.

Figure 5(a) shows the CHF values for five different mass flow rates ranging from 25 to 300 kg/s. The CHF values for the smallest mass flow are the highest at the bottom. Even higher mass flow rate than is considered in this study was shown to increase the CHF values. The CHF values for the largest mass flow rate are the greatest at the top. The large mass flow rate decreases the quality at the top, which in turn dampens the effect of the CHF decrease due to continued addition of heat from the vessel to the coolant. The associated CHFR in Fig. 5(b) also reflects the effect of the mass flow rate.

The initial subcooling of the coolant similarly affects the CHF and the CHFR as the larger mass flow rate reduces the quality at the top. In utilizing Rouge et al.' s correlation, the only effect of subcooling is fed into the calculation through input

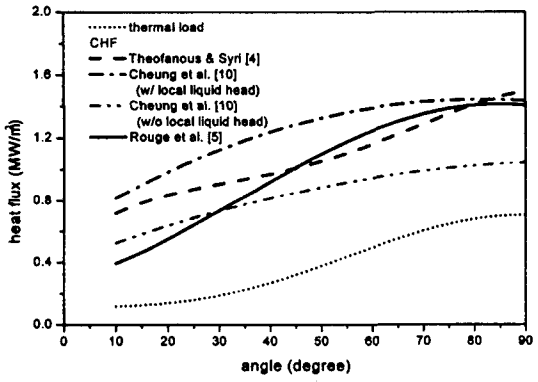

(a) CHF

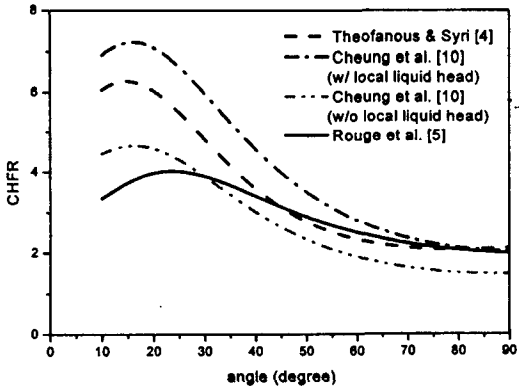

(b) CHFR

Fig. 4. CHF and CHFR Values for Different Correlations

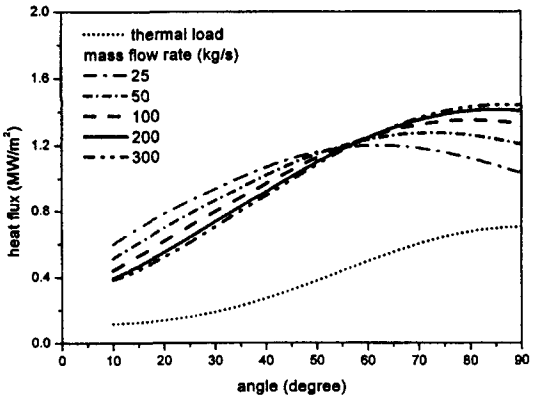

(a) CHF

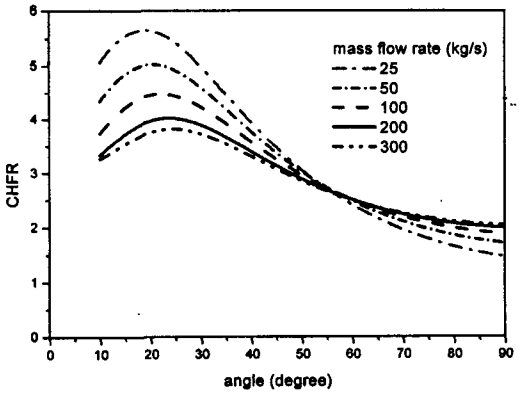

(b) CHFR

Fig. 5. Case for Differing Mass Flow Rates

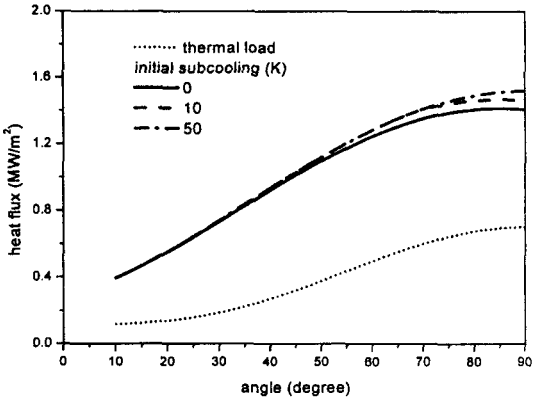

(a) CHF

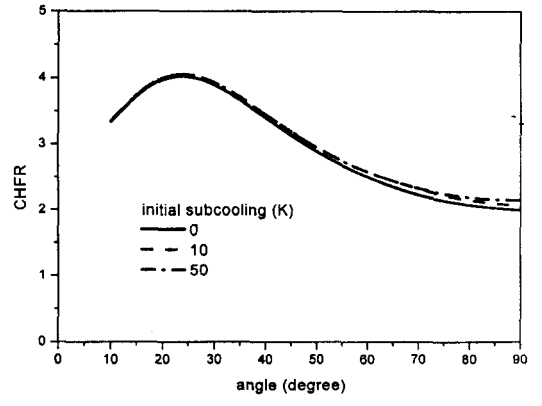

(b) CHFR

Fig. 6. Case for Forced Convective Boiling with Differing Initial Subcooling

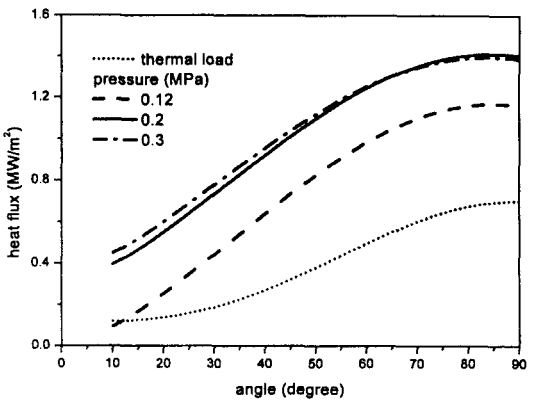

(a) CHF

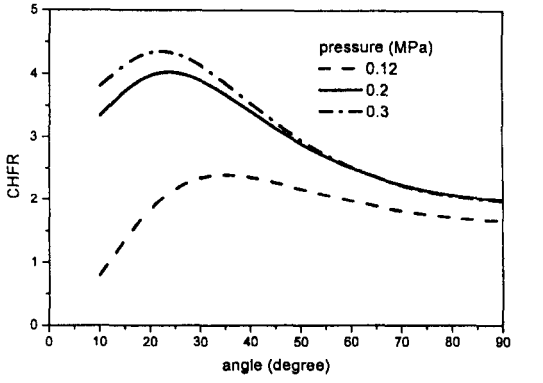

(b) CHFR

Fig. 7. Case for Forced Convective Boiling with Differing Coolant Pressures

of the initial temperature of the coolant since, as previously alluded to, the subcooling condition of the coolant is not explicitly considered in their study. The relevant CHF and CHFR values are presented in Fig. 6.

The pressure of the coolant increases the CHF at all the angular positions. But the CHF is decreased due to the relatively smaller latent heat of vaporization at the top at higher pressure. Though the local pressure is required as a function of the angular positions, the uniform pressure is assumed in this study to render the complex problem of analyzing the COASISO geometry tractable. The effect of pressure is shown for the CHF in Fig. 7(a) along with the associated CHFR in Fig. 7(b).

The gap size between the reactor vessel and the COASISO shell structure is one of the main parameters determining the CHF. The large gap increases the CHF by promoting the natural circulation within the hemispherical enclosure. On the other hand, the large gap decreases the local mass flux which has a negative impact on the CHF at high quality. The large gap increases the natural recirculation effect at the top where there is only minor forced convection effect due to the enlarged flow area at the top. Figure 8(a) shows that the local mass flux is a positive parameter at the

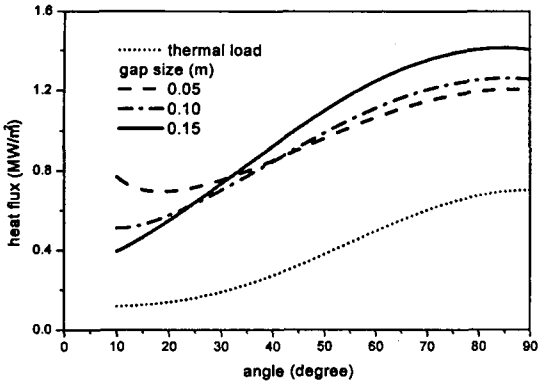

(a) CHF

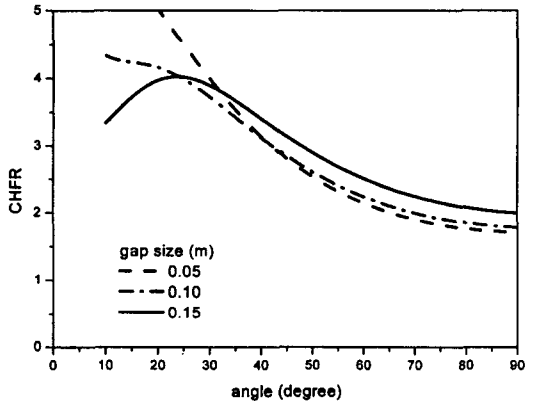

(b) CHFR

Fig. 8. Case for Forced Convective Boiling with Differing Gap Sizes

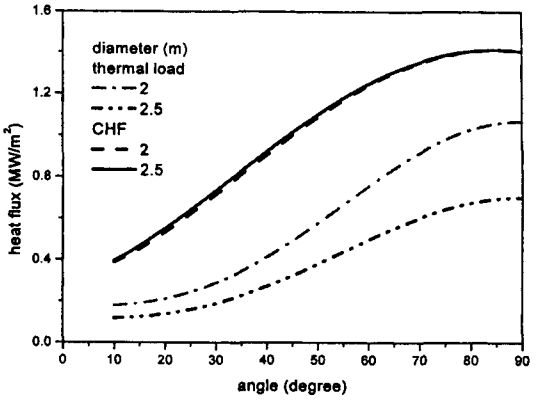

(a) CHF

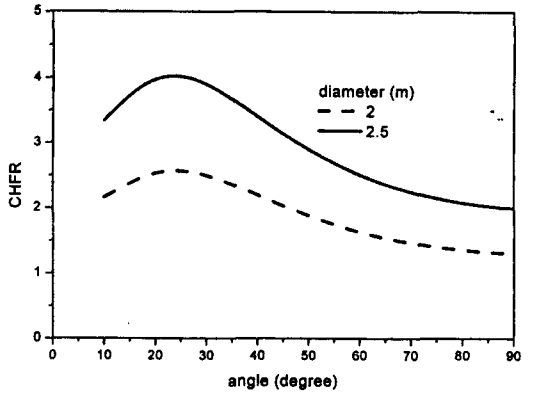

(b) CHFR

Fig. 9. Case for Forced Convective Boiling with Differing Vessel Radii

bottom where the local mass flux is large while the local quality is small. In cintrast, the large gap size is a positive parameter due to enhanced natural circulation at the top where the lcoal mass flux is small. Figure 8(b) illustrates the corresponding CHFR.

The critical paramters in determining the CHF at the top may be summarized as follows:

- The large mass velocity decreases the local quality at the top so that the CHF increases at the top
- The initial subcooling decreases the local quality at the top so that the CHF increases at the top
- The high pressure of the coolant directly increases the CHF until the decreasing latent heat of vaprorization begins to produce the counter effect above a certain limiting pressure. If the initial temperature of the coolant is constant, the higher pressure indirectly increases the CHF due to the larger initial subcooling
- The larger gap size decreases the CHF at the bottom because of the smaller local mass flux, but increases the CHF at the top because of the enhanced natural circulation effect.

The relatively smaller radius vessel increases the

thermal load at all the azimuthal positions as illustrated in Fig. 9(a). The CHF decreases due to the smaller channel flow area which increases the flow velocity given the same gap between the vessel outer wall and the COASISO because of the higher mass flux. Because Rouge et al.[5]' s correlation did not take the curved surface into account, there is little effect of the vessel radius on the CHF value. The thermal load increases on account of smaller downward heat transfer area given the same heat removal requirement. The decrease in the CHF and the increase in the thermal load render the CHFR for the vessel radius of 2 m less than that for 2.5 m as shown in Fig. 9(b).

Sensitivity analysis was performed for the heat split fraction. Figure 10(a) illustrates that the larger heat split fraction reduces the CHF as expected in upper region. Figure 10(b) shows the thermal margin for differing natural convection correlations for the downward heat transfer given the azimuthal variation of the heat flux. The result implies that the thermal margin is higher in the lower region than in the upper region. Despite increase in the removable energy moving from the bottom to the top as the inclination angle increases, the reason for the thermal margin decrease is that the local heat flux increases more rapidly moving from the bottom to the top. If the metal layer focusing effect is taken into account, more concentrated radial heat conduction will tend to decrease the CHF by virtue of the larger quality at the top.

Figure 11 demonstrates the effect of azimuthal variation utilizing different correlations on the thermal margin for the vessel. Given the same heat split fraction, the CHF values have little difference in four correlations as illustrated in Fig. 11(a). The sudden increase in the thermal load above θ = 70° per Asfia and Dhir' s [15] correlation (see Fig. 3) results in the lowest CHFR

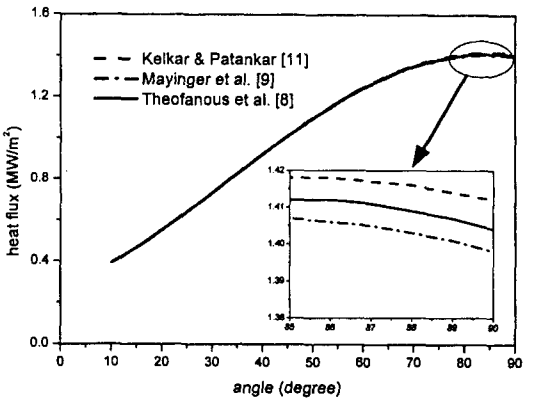

(a) CHF

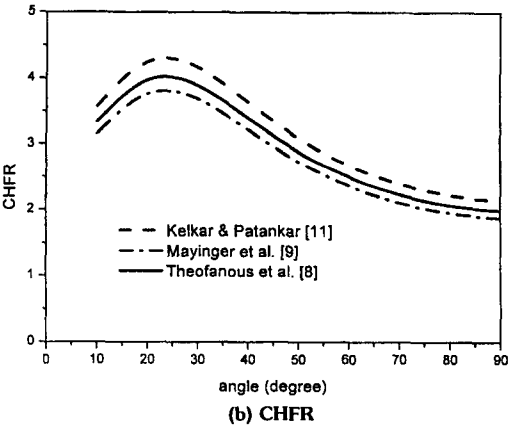

(b) CHFR

Fig. 10. Case for Forced Convective Boiling with Differing Heat Split Fractions

at the top.

In this study we have shown that the mass flux has the major influence on the CHF while the thermodynamic quality has a decreasing effect on the CHF at the top unless the limiting value is reached above which the CHF may abruptly decrease. But the change in the CHF is smaller than the change in the thermal load. The CHF value is dependent on the thermal load. The CHF standard deviations are calculated for Rouge et al.' s [5] correlation and the twelve cases of the natural convection, i.e. the combination of the three correlations [8,9,11] for the heat split times the

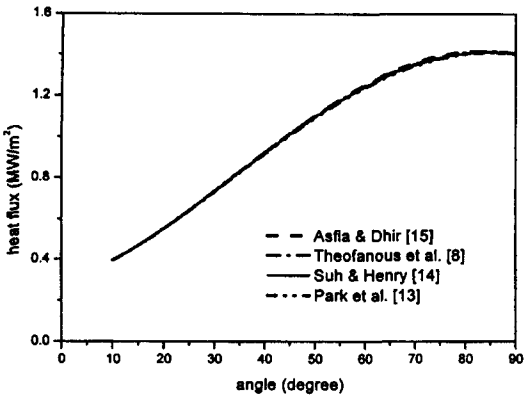

(a) CHF

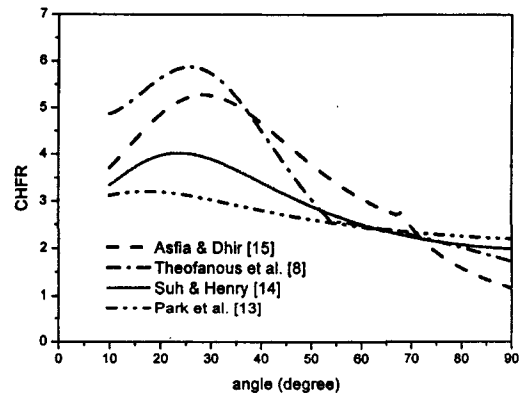

(b) CHFR

Fig. 11. Case for Forced Convective Boiling with Differing Azimuthal Distributions

four correlations [8,13,14,15] for the azimuthal distribution as listed in Table 1. The CHF standard deviation is about 10% including the error of the correlation. The standard deviation in the heat transferred downward is about 4.9%, whereas that of the azimuthal distribution is the largest, e.g. 26% at 90(, out of the factors considered in this study. Thus we may conclude that about 28% is the overall uncertainty obtained from the combination by root-sum-square (rss) of the standard deviations for the three factors. The calculation procedure is illustrated below for the standard deviations quoted in this study.

$$\sigma_{frac}^2 = \sum_{i=1}^{3} \left(frac_i - frac_{avg}\right)^2 / 3 \tag{8}$$

$$\sigma_{azi}^2 = \sum_{j=1}^{4} \left(azi_j - azi_{avg}\right)^2 / 4 \tag{9}$$

$$\sigma_{CHF}^2 = \sigma_{correlation}^2 + \sum_{i=1}^{3}\sum_{j=1}^{4} \left(CHF_{i,j} - CHF_{avg}\right)^2 / 12 \tag{10}$$

$$\sigma_{total}^2 = \sigma_{CHF}^2 + \sigma_{frac}^2 + \sigma_{azi}^2 \tag{11}$$

where the index i denotes the case of heat split fraction, and the index j signifies the case of azimuthal flux distribution.

Figure 12 shows the best-estimate, maximum, average, minimum, and the most conservative values of the CHFR for the reference mass flow rate of 200 kg/s and no initial subcooling. The best-estimate value of the CHFR is obtained when all the standard deviations of the three factors increase the CHFR. The maximum and minimum values of the CHFR cover the range of the total error. The most conservative value of the CHFR results from the case where all the standard deviations of the three factors decrease the CHFR. The values were respectively calculated as follows.

$$CHFR_{avg} = \frac{CHF_{avg}}{Q_V\left(\frac{2}{3}\pi R^3\right) frac_{avg}\, azi_{avg}} \tag{12}$$

$$CHFR_{best} = CHFR_{avg} \frac{1+\sigma_{CHF}}{(1-\sigma_{frac})(1-\sigma_{azi})} \tag{13}$$

$$CHFR_{max} = CHFR_{avg}\left(1+\sigma_{total}\right) \tag{14}$$

$$CHFR_{min} = CHFR_{avg}\left(1-\sigma_{total}\right) \tag{15}$$

$$CHFR_{worst} = CHFR_{avg} \frac{1-\sigma_{CHF}}{(1+\sigma_{frac})(1+\sigma_{azi})} \tag{16}$$

Table 4. Standard Deviations* for Heat Split, Azimuthal Profile and Forced Convection CHF

Angular Position	30°	40°	50°	60°	70°	80°	90°
Heat Split Fraction	4.90	4.90	4.90	4.90	4.90	4.90	4.90
Azimuthal Distribution	25.75	21.07	12.68	8.31	2.88	14.21	26.03
CHF (25 kg/s)	0.57	0.98	1.39	1.75	2.03	1.65	1.72
CHF (50 kg/s)	0.42	0.69	0.97	1.14	1.34	1.15	1.31
CHF (100 kg/s)	0.20	0.46	0.61	0.71	0.79	0.67	0.80
CHF (200 kg/s)	0.18	0.30	0.37	0.43	0.46	0.40	0.47
CHF (300 kg/s)	0.14	0.23	0.29	0.31	0.34	0.28	0.33

* unit: % (not including the error of the correlation itself)

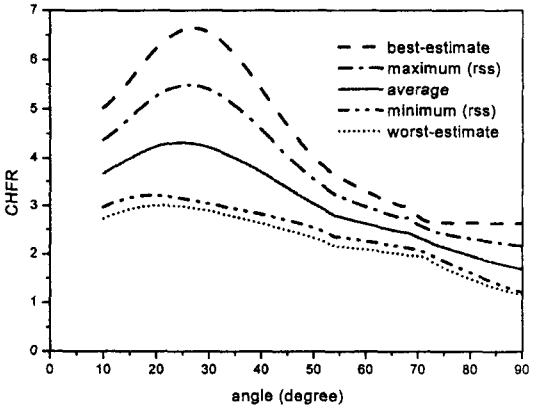

Fig. 12. CHFR Value Uncertainty Band for Various Cases

The standard deviations for the three factors, respectively, are provided at the angles of 30°, 40°, 50°, 60°, 70°, 80° and 90° in Table 4 for mass flow rates ranging from 25 to 300 kg/s. Observe that the larger the mass flow rate of the coolant, the smaller the standard deviation in the CHF values. This is because the higher mass flow tends to decrease the quality, which in turn reduces the standard deviation in terms of the CHF. The standard deviations of the azimuthal flux distribution are large at the top and at the bottom.

4. Conclusions and Future Work

In this study we have shown that principal factors affecting the thermal margin calculation are the amount of heat to be transferred downward from the molten pool, variation of heat flux with the angular position, and the amount of removable heat by external cooling. Relevant models and correlations were critically reviewed and applied in terms of their capabilities and uncertainties in estimating the thermal margin of the vessel to failure on account of the CHF. Results of the thermal margin calculation were statistically treated and the associated uncertainties were quantitatively assessed to identify the remaining issues deserving further study in the near term. Our results indicated a higher thermal margin at the bottom than at the top of the vessel accounting for the natural convection within the hemispherical molten debris pool within the lower head.

Main conclusions from this study may be summarized as follows. First, the natural convection (i.e. downward versus upward heat transfer, and the azimuthal heat flux distribution) in the molten pool is the parameter of utmost

importance in determining the CHFR. Especially, the azimuthal heat flux profile from the molten pool turns out to be the main parameter. However, existing experimental and numerical studies appear to yield rather differing results judging from the large standard deviations computed in this study. The variation of this magnitude may have significant impact on the CHFR. Further study is needed to fully test and comprehensively theorize the natural convection in the molten pool. Second, Rouge et al.'s correlation did not unfortunately cover the local subcooled condition and the curved surface. Experiments for the CHF in the forced convective boiling need to be performed to take the effect of the downward facing curved surface into consideration.

Sensitivity analysis must further be performed to account for the metal layer focusing effect, and multidimensional heat conduction, melting and ablation in the vessel wall. In particular, the metal layer focusing effect will tend to decrease the CHFR because more localized radial heat will have to be removed from the vessel wall in contact with the metal layer.

The information obtained from this study will help identify as quantitatively as possible the maximum heat removal capability and limitations of this novel technology of COASISO during the course of engineering design of the IVR structure for next generation reactors.

Acknowledgement

The authors are grateful for technical discussion with the experts of the Korea Atomic Energy Research Institute, the Korea Institute of Nuclear Safety, the Korea Advanced Institute of Science and Technology, and the KEPCO Electric Power Research Institute during the course of this work.

Nomenclature

A	function in Rouge et al.'s [5] correlation, Eq. (5)
$A_{channel}$	local channel area of the COASISO
A_{heated}	local heating surface area of outer vessel surface
avg	average value
azi	azimuthal heat flux distribution
B	function in Rouge et al.'s [5] correlation, Eq. (5)
C	function in Rouge et al.'s [5] correlation, Eq. (5)
CHF	critical heat flux
$CHFR$	critical heat flux ratio
D	function in Rouge et al.'s [5] correlation, Eq. (5)
E	function in Rouge et al.'s [5] correlation, Eq. (5)
e	gap between the COASISO shell structure and the reactor vessel
F_{Ja}	function in Cheung et al. [10] correlation, Eq. (4)
F_{Lb}	function in Cheung et al. [10] correlation, Eq. (4)
F_P	function in Cheung et al [10] correlation, Eq. (4)
$F_\bullet$	function in Cheung et al [10] correlation, Eq. (4)
$frac$	heat split fraction
G	local mass flux
g	gravitational acceleration
H	pool height
h_f	enthalpy of the saturated liquid
h_{fg}	latent heat of vaporization
h_{in}	initial enthalpy of the coolant
k_p	thermal conductivity
$\dot{m}$	mass flow rate
N_u	Nusselt number

p pressure
Q_v volumetric heat generation rate
q''_{act} actual heat flux or thermal load
q''_{CHF} critical heat flux
$q''_{down.avg}$ average downward heat flux from the vessel lower head
R vessel radius
Ra' Rayleigh number

Greek Letters

α_p thermal diffusivity
β volumetric expansion coefficient
x local thermodynamic quality
ν_p kinematic viscosity
θ azimuthal angle
σ standard deviation

References

1. I. S. Hwang et al., "In-Vessel Retention against Water Reactor Core Melting Accidents," Submitted for Publication in *Nuclear Technology*, June (2000).
2. Z. Guo and M. S. El-Genk, "An Experimental Study of Saturated Pool Boiling from Downward Facing and Inclined Surfaces," *Int. J. Heat Mass Transfer*, 35, 9, 2109 (1992).
3. M. S. El-Genk and A. G. Glebov, "Transient Pool Boiling from Downward-facing Curved Surface," *Int. J. Heat Mass Transfer*, 38, 12, 220 (1995).
4. T. G. Theofanous and S. Syri, "The Coolability Limits of a Reactor Vessel Lower Head," *Nuclear Engineering and Design*, 169, 59 (1997).
5. S. Rouge, I. Dor and G. Geffraye, "Reactor Vessel External Cooling for Corium Retention SULTAN Experimental Program and Modeling with CATHARE code," Workshop on In-Vessel Core Debris Retention and Coolability, Garching, Germany, March 3-6 (1998).
6. J. W. Park and D. W. Jeong, "An Investigation of Thermal Margin for External Reactor Vessel Cooling (ERVC) in Large Advanced Light Water Reactor (ALWR)," Proc. of the Korean Nuclear Society Spring Meeting, Kwangju, Korea, 1, 473 (1997).
7. U. Steinberner and H. H. Reineke, "Turbulent Buoyancy Convection Heat Transfer with Internal Heat Sources," Proc. of the Sixth Int. Heat Transfer Conference, Toronto, Canada, August (1978).
8. T. G. Theofanous et al., "In-vessel Coolability and Retention of a Core Melt," DOE/ID-10460, vol 1, U.S. Department of Energy, Washington, DC, USA (1995).
9. F. Mayinger, M. Jahn, H. H. Reineke and U. Steinberner, "Examination of Thermohydraulic Process and Heat Transfer in a Core Melt," Final report BMFT RS 48/1, Technical University, Hannover, Germany (1975).
10. F.B. Cheung, K. H. Haddad and Y. C. Liu, "Critical Heat Flux Phenomenon on a Downward Facing Curved Surface," NUREG/CR- 6507 PSU/ME-97-7321 (1997).
11. K. M. Kelkar and S. V. Patankar, "Computational Modeling of Turbulent Natural Convection in Flows Simulating Reactor Core Melt," Innovative Research, Inc., Final Report submitted to SNL, Albuquerque, NM, USA (1993).
12. O. Kymalainen, H. Tuomisto, and T. G. Theofanous, "Heat Flux Distribution from a Volumetrically Heated Pool with High Rayleigh Number," Proc. of the Sixth Nuclear reactor Thermal Hydraulics (NURETH-6), Grenoble, France (1993).
13. H. J. Park, V. K. Dhir and W. E. Kastenberg, "Effect of External Cooling on the Thermal Behavior of a Boiling Water Reactor Vessel

Lower Head," *Nuclear Technology*, 108, 266-282 (1994).

14. K. Y. Suh and R. E. Henry, "Integral Analysis of Debris Material and Heat Transport in Reactor Vessel," *Nuclear Engineering and Design*, 151, 203 (1994).
15. F. J. Asfia and V. K. Dhir, "An Experimental Study of Natural Convection in a Volumetrically Heated Spherical Pool with Rigid Wall," Int. Mechanical Engineering Congress & the Winter Annual Meeting, Chicago, IL, USA, November 6-11 (1994).
16. S. H. Yang, W. P. Baek and S. H. Chang, "An Analysis of Critical Heat Flux on the External Surface of the Reactor Vessel Lower Head," Proc. of the Korean Nuclear Society Autumn Meeting, Seoul, Korea October 29-30 (1999).